

TR/BR-23/99-2000

MODELLING OF SURFACE RUNOFF, INFILTRATION AND EVAPOTRANSPIRATION




**NATIONAL INSTITUTE OF HYDROLOGY
JALVIGYAN BHAWAN
ROORKEE - 247 667 (UTTARANCHAL)**

1999-2000

Preface

The present report is the part of the Hydrology Project concerned with the Estimation of irrigation return flow in Lokapavani area of KR Sagar command in Karnataka. In this project, Numerical model for surface and subsurface flow with sink term for evapotranspiration from crop has to be developed to estimate the irrigation return flow from the irrigated field. The return flow may amount to as much as 20% to 40% of the volume of water applied for irrigation. In absence of any studies, it is usually taken as 35% of the water applied for irrigation in case of canal irrigation and 30% in case of irrigation from ground water applied to small segments of irrigation commands. Estimation of irrigation return flow, which is one of the most significant components of water balance in irrigation command areas, is a complex problem and its solution requires a detailed water balance in the study area. In applying irrigation water, crop needs and extractions can be matched evenly. In such cases, the irrigation return flow depends on local soil characteristics, the meteorological parameters, method of irrigation, types of crop grown and depth to water table. The irrigation return flow should be computed for each soil group and crop type at micro level through soil moisture modelling.

In this study, a model has been developed considering surface flow component and subsurface flow component along with the evapotranspiration from the crop as the sink term. The surface flow component is represented using one-dimensional St. Venant equations and the subsurface flow component is represented using one-dimensional Richards equation with the sink term for the evapotranspiration crop. These equations are solved numerically. This report is prepared by Dr. Vivekanand Singh, Scientist "B" of the Institute.


(K S Ramasastri)
Director

CONTENT

PREFACE.....	II
CONTENT.....	III
LIST OF FIGURES.....	IV
ABSTRACT.....	V
1.0 INTRODUCTION.....	1
2.0 GOVERNING EQUATIONS.....	6
2.1 SURFACE FLOW EQUATIONS:.....	6
2.2 SUBSURFACE FLOW EQUATION.....	7
3.0 NUMERICAL METHOD.....	10
3.1 SURFACE FLOW.....	10
3.1.1 <i>Initial Conditions</i>	13
3.1.2 <i>Boundary Conditions</i>	13
3.1.3 <i>Stability Condition</i>	15
3.2 SUBSURFACE FLOW.....	15
3.2.1 <i>Initial Conditions</i>	18
3.2.2 <i>Boundary Conditions</i>	18
3.3 CALCULATION OF EVAPOTRANSPIRATION (SINK TERM).....	19
3.3.1 <i>Variation of Evapotranspiration with Soil Moisture</i>	19
3.4 SURFACE AND SUBSURFACE FLOW INTERACTION.....	21
3.4.1 <i>Boundary Conditions</i>	21
3.4.2 <i>Soil Moisture Characteristics</i>	22
4.0 RESULTS AND DISCUSSION.....	23
4.1 SIMULATION OF HYPOTHETICAL CASE STUDY.....	23
4.1.1 <i>Subsurface Flow with Sink</i>	23
4.1.2 <i>Surface and Subsurface Flow with Sink</i>	31
5.0 CONCLUSION.....	36
REFERENCES.....	37

List of Figures

Fig. 1	Finite-Difference Grid for Surface Flow	10
Fig. 2	Finite-Difference Grid for Subsurface Flow	16
Fig. 3	Definition Sketch of Pressure Head type Boundary Condition	18
Fig.4	Plant Root Uptake Function E_a with Soil Moisture	20
Fig. 5	Movement of Moisture Front below Ground Surface in Advance Phase	24
Fig. 6	Movement of Moisture Front below Ground Surface in Recession Phase	25
Fig. 7	Moisture Content Profile in next irrigation (Advance & Recession)	26
Fig. 8	Variation of Sink Term along depth for Advance Phase	26
Fig. 9	Variation of Sink Term along depth for Recession Phase	27
Fig. 10	Sink Term after second Irrigation along depth for Advance & Recession	27
Fig. 11	Moisture Profiles with & without Sink Term at different time along depth (Advance)	28
Fig. 12	Moisture Profiles with & without Sink Term at different time along depth (Recession)	29
Fig. 13	Moisture Profiles with Sink Term for Constant Head at different time along depth (Advance)	30
Fig. 14	Variation of Sink Term (evapotranspiration) along the Depth and Time	31
Fig. 15	Time of Water Arrival along the Length of the Field	32
Fig. 16	Surface Water Depth and Wetting Front at different time (Advance Phase)	33
Fig. 17	Position of the Surface Water Depth and Wetting Front at different Time (Recession Phase)	33
Fig. 18	Movement of Moisture Content along depth at different Time	34
Fig. 19	Variation of Sink term along Depth at different Time	35

ABSTRACT

In this study, a model has been developed considering surface flow component and subsurface flow component along with the evapotranspiration from the crop as the sink term. The surface flow component is represented using one-dimensional St. Venant equations and the subsurface flow component is represented using one-dimensional Richards equation with the sink term for the evapotranspiration from crop. The sink term is calculated considering the crop coefficient, potential evaporation, the moisture content in the root zone and the distribution of the root density along the root zone depth. The surface flow equations are solved by the second order accurate, explicit, essentially-non-oscillating (ENO) finite difference scheme. The advance and recession fronts are treated in the same way as regular interior points. The strongly implicit procedure is used to solve the subsurface flow equation. Two models have been developed. First model is developed using the subsurface flow component only with the sink term. Second model is developed for all processes in a cropped field, such as surface flow and subsurface flow components along with the sink term for evapotranspiration from the crop and the return flow generated below the ground surface.

A hypothetical problem has been simulated with the synthetic data set. First model has been used to simulate the subsurface flow component with the sink term having the ponded water depth at the surface with variable head (sugar cane) and with constant head (paddy). Second model has been used to simulate the surface flow and subsurface flow components along with the sink term for evapotranspiration from crop. The results obtained from these models have been presented for the variable and constant heads and with and without sink term. The effect of the sink term has been shown for the applicability of the model. The percentage of the return flow from the irrigation has also been given.

1.0 INTRODUCTION

The economy of an agriculturally based country largely depends upon agriculture. Though the country is provided with vast resources of land and water, it suffers from low crop yields and is hardly able to meet the food requirements of its ever-increasing population.

Water resources play a dominant role in the agricultural development and ecological balance. Unfortunately this resource is finite and its usages have been very wasteful despite implementation of several water management programs in the country. The actual water utilized in agriculture is approximately one-third of the total utilizable surface and ground water resources. There is a distinct need for a review and proper planning for the optimal utilization of water stored in the soil.

The soil-plant-atmosphere continuum is very complicated system. Current approaches to problems involved in the study of this system are based on the recognition that it is a physically integrated, dynamic system in which various flow processes occur interdependently like links in a chain. The universal principle, which operates consistently through out the system is that water flow always takes place spontaneously from regions of higher to regions of lower potential energy. The very occurrence of differences or gradients of potentials between locations in the system constitutes the force that induces the flow within and between the soil, the plant and the atmosphere. The water transport phenomena within the soil-plant-atmosphere continuum, which plays a central part in the terrestrial sector of the hydrologic cycle and in irrigated agriculture are infiltration, drainage, retention of water in soil and evapotranspiration from the crops. These processes required to be solved with the help of the surface flow and subsurface flow components along with the evapotranspiration from the crops. With the availability of computer, simulation of these water transfer phenomena within the system became feasible.

Analysis of unsteady shallow water flow over a porous medium with sink term is required to determine depths, velocities, runoff hydrographs, infiltration and evapotranspiration in the design of surface irrigation systems. Surface irrigation is, in many cases, the cheapest way of irrigating plane agricultural lands. In this method, water is applied at the higher end of the field and flows by gravity towards the lower end. The main objective of the surface irrigation is to provide enough water to soil moisture storage to maintain plant growth until the next irrigation. The frequency of irrigation is dependent upon the moisture retention capacity of the soil, the evapotranspiration rate and the stage of crop growth, but it is desirable to maintain as long a time interval between irrigations as possible to lower labour costs. If the

surface irrigation is intensive, water would percolate below the root zone depth and reach the local water table. An excessive amount of such percolated water is wasteful and may lead to drainage problems. On the other hand, if less amount is supplied, then the plant would be subjected to moisture stress before the next irrigation and yield will be reduced. An optimum supply to the root zone is needed for greatest yield. The amount of water that infiltrates into the soil depends on the total amount of water supplied at the upstream end of the field, the soil conditions and the types of crop in the field. The crops such as sugarcane and paddy require more irrigation water from which there is more runoff and deep percolates. These deep percolations join the water table below the root zone and termed as the return flow from irrigation. Hydraulic analysis of surface flow and subsurface flow with sink term during all the phases of irrigation from advance to recession is important for successful design and operation of a surface irrigation system. These systems should be designed and operated in such a way that the excess runoff at the downstream outlet and excess deep percolation below the root zone are minimized (Michael 1978).

The return flow may amount to as much as 20% to 40% of the volume of water applied for irrigation. In absence of any studies, it is usually taken as 35% of the water applied for irrigation in case of canal irrigation and 30% in case of irrigation from ground water applied to small segments of irrigation commands. Estimation of irrigation return flow, which is one of the most significant components of water balance in irrigation command areas, is a complex problem and its solution requires a detailed water balance in the study area. When irrigation water is supplied from ground water reservoir, the water is applied without conveying it over long distances and the transmission loss is small. In applying groundwater, crop needs and extractions can be matched evenly. In such cases, the irrigation return flow depends on local soil characteristics, the meteorological parameters, method of irrigation, types of crop grown and depth to water table. The irrigation return flow should be computed for each soil group and crop type at micro level through soil moisture modelling.

Advances in computers have made it feasible to apply numerical techniques for solving complex systems of equations. This has given rise to increased efforts to develop numerical models for analyzing surface irrigation systems (Katopodes and Strelkoff 1977a, Playan et al. 1994a). Numerical modeling of flow in a surface irrigation system is complicated because of (i) the presence of a source term in the continuity equation and (ii) the existence of an advance or recession front. Traditionally, characteristic methods and implicit finite-difference methods are used for solving the governing shallow water flow equations along with an empirical equation for the infiltration. Advancing front in these models is treated as a moving downstream boundary and approximate volume balance methods are used

for finding the advance rate of the tip. These methods are cumbersome and it is difficult to extend them for two-dimensional flow case, which may occur in a basin irrigation system. Explicit finite-difference methods for solving the shallow water equations are easier to implement than the schemes based on the method of characteristics (Chaudhry 1993). However, a finite-difference scheme with fixed cell size may result in a negative flow depth, especially near the advancing front. This occurs when the volume to be infiltrated becomes more than the volume supplied to the node by the surface flow. This may necessitate the use of a small grid size in the finite-difference models, which results in increased computational cost. The above aspect should be considered while developing finite-difference based numerical models for surface irrigation.

Most of the earlier full dynamic models are based on the method-of-characteristics (Kincaid et al. 1972, Bassett 1972, Sakkas and Strelkoff 1974, Bassett and Fitzsimmons 1976, and Katopodes and Strelkoff 1977). These models require special numerical treatment in the region of the advancing front where the flow depth rapidly approaches zero and the characteristics are strongly curved. All these models treat the advancing front as the downstream boundary and use the volume balance approach to advance the tip (Katopodes and Strelkoff 1977). The finite-difference methods for solving the Saint-Venant equations are easier to implement than the schemes based on the method-of-characteristics and therefore, have become more popular (Chaudhry 1993). Wallender and Rayej (1990) and Bautista and Wallender (1992, 1993) developed surface irrigation models based on the implicit Preissman scheme. These models also treat the advancing front as the downstream boundary. The shooting method is used to obtain the intake opportunity time for a given advance distance. These models become complicated and computationally intensive if a quasi-analytical method is used for computing the infiltration. It is also not easy to extend these models for two-dimensional applications.

Numerical simulation of surface irrigation in cropped land is complicated because the surface flow equations need to be solved under varying irrigation supply and infiltration, and for realistic upstream and downstream boundary conditions. The surface flow hydraulics should be modeled using two-dimensional shallow water flow equations if the catchment slope and roughness are randomly distributed, but in this study, one-dimensional equations are used. Numerical modelling of surface irrigation in cropped field becomes even more complicated because theoretically, the process is described by a conjunctive surface-subsurface flow system with sink term (evapotranspiration). The surface and subsurface flow components are in dynamic equilibrium and they interact through the process of infiltration at the ground surface. The unsaturated subsurface flow hydraulics in such a model is described

by the Richards equation, if the return flow below the root zone has to be ascertained. Difficulties are encountered in the numerical solution of Richards equation when the subsoil characteristics vary in a complicated way for a non-homogeneous system (Celia et al. 1990). Two-dimensional Richards equation might have to be considered in such a case, but in this study one-dimensional Richards equation has been considered for homogeneous system.

A surface irrigation model based on an explicit finite-difference method would be more flexible than an implicit finite-difference model for handling different types of infiltration equations. It can also be easily implemented for two-dimensional flow. In such a model, the treatment is the same for all the grid points located between the two ends of the field. The advancing front need not be treated as the downstream boundary. Playan et al. (1994) presented an explicit two-dimensional model for basin irrigation, based on a variation of the Leapfrog finite-difference scheme. In this model infiltration is calculated using the empirical equation. It should be noted here that a finite-difference scheme with fixed cell size may result in negative flow depths, especially near the advancing front. This occurs when the volume to be infiltrated becomes more than the volume supplied to the node by the surface flow. Playan et al. (1994) allowed the infiltration to occur only when the flow depth is greater than a minimum specified value and also adjusted the intake opportunity time at a node to avoid the above problem.

All the earlier models of surface irrigation used the empirical Kostiakov equation for determining the infiltration rate. The empirical Kostiakov parameters are influenced by (i) soil characteristics (ii) soil moisture (iii) geometry of the channel (iv) measurement technique etc. The effect of surface flow depth on the infiltration rate is not considered. Parlange et al. (1985) introduced an infiltration equation, which has the advantage of using parameters that are related to soil properties. These parameters do not depend on the particular conditions under which they are evaluated i.e. duration of the test, number of data points, etc. Schmitz et al. (1985) developed a hydrodynamic border irrigation model with infiltration computed with the Parlange equation. They solved the surface flow equations using the implicit characteristic method. This makes it necessary to use an iterative procedure for coupling the surface flow with the infiltration equation because the infiltration rate in the Parlange equation is depth dependent. The return flow from applied irrigation or rainfall below the root zone can only be simulated using the Richards equation with the sink term. The downward flux at any depth can be estimated with the help of the Richards equation.

There are several methods of estimating the return flow below root zone. First method is the distributed model, which solves the Richards equation for unsaturated soil. Second is

the soil moisture accounting model, in which the entire unsaturated zone is considered as a unit. These models involve many restrictive assumptions relating to the flow process. Prominent among them is the field capacity, which must be quantified as a flow parameter. Chandra, (1979) has pointed out that soil moisture accounting models involve a book keeping of various mass balance components of the unsaturated zone. While the distributed model based on Richards equation requires more computational effort and more expertise. Miller (1964) observed that the field capacity corresponding to the 0.33 bar tension can not be taken as the reasonable measure. Mohan Rao et al. (1990) developed a soil moisture accounting model taking into account the estimation of field capacity. Author has given a method for estimating field capacity as a flow parameter but this method is more suitable for coarse soils. The distributed models (based on the solution of the Richards equation) are free from many of the restricted assumptions associated with the SMA model.

The main objective of this study is to develop a model considering surface flow and subsurface flow components along with the evapotranspiration from the crop as the sink term.

In this study, a model has been developed considering the surface flow component and subsurface flow component with the evapotranspiration from the crop as the sink term. The surface flow is represented by one-dimensional St. Venant equations and the subsurface flow is represented by Richards equation with the sink term for the evapotranspiration. The sink term is calculated by considering the crop coefficient, potential evaporation, the moisture content in the root zone and the distribution of the root density along the root zone depth. The surface flow equations are solved by the second order accurate, explicit, essentially-non-oscillating (ENO) finite difference scheme. This model is simpler to implement and is computationally more efficient than the surface irrigation model based on the Leapfrog scheme and implicit schemes. Advance and recession fronts are treated in the same way as regular interior points. The strongly implicit procedure is used to solve the subsurface flow equation. Both the components are simultaneously solved and interacting through the process of infiltration at the ground surface.

2.0 GOVERNING EQUATIONS

Mathematical modelling of surface runoff, infiltration and evapotranspiration involves the solution of the governing equations for the flow processes of surface, subsurface and evapotranspiration. In this study, the surface flow is represented by one-dimensional St. Venant equations in the x-direction with source term in continuity equation. The subsurface flow as the movement of soil moisture in unsaturated zone is represented by the one-dimensional Richards equation in the mixed based form in z direction with the sink term to account the evapotranspiration from the crops. The evapotranspiration is computed using the empirical equation, which is described later.

2.1 Surface Flow Equations:

Surface flow is assumed to occur in a prismatic channel of rectangular section. The one-dimensional St Venant equations in conservation form for such a case are given by: (Chaudhry, 1993);

Continuity equation

$$\frac{\partial h}{\partial t} + \frac{\partial q}{\partial x} = (R - I) \quad (1)$$

Momentum Equation

$$\frac{\partial q}{\partial t} + \frac{\partial}{\partial x} \left[\frac{q^2}{h} + \frac{g h^2}{2} \right] = g h (S_o - S_f) \quad (2)$$

Equations (1) and (2) can also be written in vector forms as:

$$\frac{\partial U}{\partial t} + \frac{\partial F}{\partial x} = S \quad (3)$$

in which, U, F and S are vectors and are given as

$$U = \begin{Bmatrix} h \\ q \end{Bmatrix}, F = \begin{Bmatrix} q \\ \frac{q^2}{h} + \frac{g h^2}{2} \end{Bmatrix} \text{ and } S = \begin{Bmatrix} (R - I) \\ g h(S_o - S_f) \end{Bmatrix} \quad (4)$$

where, h = depth of flow (m); q = discharge per unit width (m^2/s); R = volumetric rate of rainfall per unit surface area (m/s); I = volumetric rate of infiltration per unit area (m/s); S_o = bottom slope in the direction of flow; S_f = friction slope; g = acceleration due to gravity (m/s^2); x = distance along the flow direction (m) and t = time (s). The derivation of the above equations has been reported by Chaudhry (1993). The assumptions in deriving the above equations are as follows:

1. The pressure distribution is hydrostatic. This is true if the vertical acceleration is small, i.e. if the streamlines do not have sharp curvatures.
2. The slope, q , of the channel bottom is small so that $\sin q \approx \tan q$ and $\cos q \approx 1$.
3. The velocity distribution along the depth is uniform.
4. The channel is straight and prismatic.
5. The transient-state friction losses may be computed using formulae for the steady-state friction losses.

The friction slope can be computed using the Manning equation. The Manning equation for computing the friction slope is given by

$$S_f = \frac{(qn)^2}{h^{3.33}} \quad (5)$$

where, n Manning's roughness coefficient

2.2 Subsurface Flow Equation

The subsurface flow is considered as one-dimensional motion of a single-phase incompressible fluid. The one-dimensional, transient, unsaturated flow equation in an isotropic porous medium is derived by applying the principle of conservation of mass and the basic Darcy's law for unsaturated flow and making the following assumptions:

- (i) Compressibility of the medium and the water are negligible, and
- (ii) The air phase is stagnant and is at atmospheric pressure.

The one-dimensional continuity equation with sinks term within the flow domain is written as (Freeze & Cherry, 1979):

$$\frac{\partial \theta}{\partial t} + \frac{\partial V_z}{\partial z} = Si(z, t) \quad (6)$$

in which, θ = volumetric moisture content; V_z = Darcy flow velocities in z direction, Si = Sink term representing the rate of withdrawal of water per unit volume of the soil; and z is distance along z-direction and is taken positive down wards. It is assumed that the Darcy's law is applicable for evaluating the velocity components. The Darcy's law for unsaturated flow in z directions for an isotropic soil is

$$V_z = -K(\psi) \left(\frac{\partial \psi}{\partial z} - 1 \right) \quad (7)$$

in which, ψ = pressure (suction) head (m); and $K(\psi)$ = unsaturated hydraulic conductivity (m/s); which depends on the suction head, ψ . Substitution of Equation (7) in Equation (6) yields the Richards equation (Freeze and Cherry, 1979):

$$\frac{\partial \theta}{\partial t} = \frac{\partial}{\partial z} \left[K(\psi) \left(\frac{\partial \psi}{\partial z} - 1 \right) \right] \quad (8)$$

Equation (8) is said to be in "mixed form" since it includes both the dependent variables θ and ψ . Most of the earlier studies on unsaturated ground water flow have employed the Richards equation in either pressure head form or moisture content form. The pressure head form of the Richards equation is applicable to the flow in saturated and unsaturated zones and layered zones, but gives large mass balance errors. The moisture content form of the Richards equation perfectly conserves the mass within the flow domain, but is not applicable to the saturated flow zones and is not directly applicable to the layered zones because of the discontinuities in moisture content profiles at the interface of layers. These difficulties are over come by using the mixed form of Richards equation. The mixed form of Richards equation results better numerical behaviours then the other forms [Allen and Murphy (1986), Hill et al. (1989) and Celia et al. (1990)]. It combines the benefit of both the pressure head and moisture content forms of Richards equation. The numerical models based on the mixed form of Richards equation can guarantee mass balance while having no limitations when applied to field problems (Singh and Bhallamudi, 1998). The main difficulty in the Richards equation to actual field situations is the estimation of the parameters of the

soil characteristic curves. Characteristics relationships between the suction head, ψ and the hydraulic conductivity, K (ψ - K relationship) and between the moisture content, θ and the suction head, ψ (ψ - θ relationship) are needed while solving Eqs. (6) and (7) in the unsaturated zone. In general, ψ - K and ψ - θ relationships are not unique and soils exhibit different behaviour during wetting and drying phases. This hysteresis in soil characteristics is not considered for the cases studied in the present work. However, the hysteresis can be included by employing different ψ - K and ψ - θ relationships for wetting and drying processes. Several quasi-analytical equations are available to describe ψ - K and ψ - θ relationships in Rawls and Brakensick, (1988).

3.0 NUMERICAL METHOD

3.1 Surface Flow

Surface flow equations constitute a set of non-linear hyperbolic partial differential equations. A recently developed high resolution Essentially Non-Oscillating (ENO) scheme for solving the shallow water flow equations (Nujic, 1995) has been employed in the present study to solve the surface flow equations. The scheme, proposed by Nujic (1995), has been suitably modified by Singh and Bhallamudi (1996), to account for the non-zero source term in the continuity equation. This scheme, unlike many other classical second-order accurate schemes such as the MacCormack method, is non-oscillatory even when sharp gradients in the flow variables are present. The main advantages of this scheme are its simplicity, ease of implementation and ease of extension to two-dimensional case. It is an explicit, two-step predictor-corrector scheme, which results in second-order accuracy in both space and time. A detail description of the method as applied in the present study is outlined in Singh and Bhallamudi (1996). Only the predictor and corrector parts have been reproduced here. The two independent variables, x and t divide the x - t plane into a grid as shown in Fig. 1. The grid interval along the x -axis is Δx and the grid interval along the t -axis is Δt . To refer to different variables at grid points the number of the spatial grid is used as a subscript and that of the time grid as a superscript. For example the variable U_i^n represents at the i^{th} spatial grid point and n^{th} time grid point.

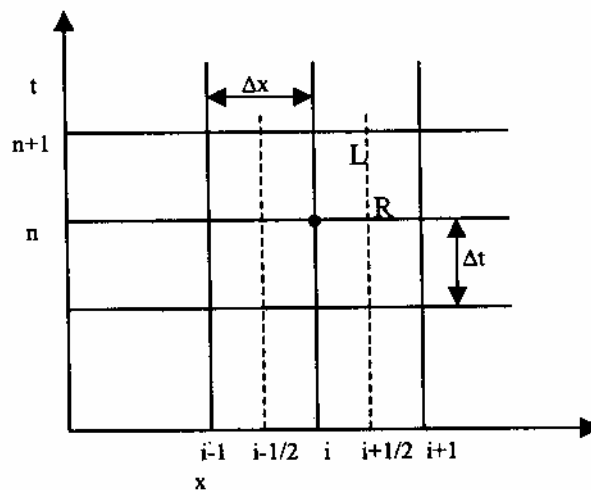


Fig. 1 Finite-Difference Grid for Surface Flow

The finite-difference analog of the Eq. (3) is written here for a finite-difference grid where the subscript i refers to the grid point in the x -direction and the superscripts n and $*$ refer to the values at the known time level and the predictor level, respectively.

The finite-difference form of Eq. (3) for the explicit determination of U_i^* is written as

$$U_i^* = U_i^n - \frac{\Delta t}{\Delta x} \left[F_{i+\frac{1}{2}}^n - F_{i-\frac{1}{2}}^n \right] + \Delta t S_i^n \quad (9)$$

where, $F_{i+\frac{1}{2}}^n$ represents the numerical flux through the cell face between nodes i and $i+1$. Δx is the grid spacing and Δt is the computational time step. The numerical flux is given as

$$F_{i+\frac{1}{2}}^n = \frac{1}{2} \left[F_R^n + F_L^n - \alpha (U_R^n - U_L^n) \right] \quad (10)$$

in where, $\alpha =$ a positive coefficient, $F_R = f(U_R) =$ the flux computed using the information from the right side of the cell face and $F_L = f(U_L) =$ the flux computed using the information from the left side of the cell face. U_R and U_L are obtained using the following equation.

$$U_L = U_i + \frac{1}{2} \delta U_i \quad \text{and} \quad U_R = U_{i+1} - \frac{1}{2} \delta U_{i+1} \quad (11)$$

There are several ways to determine δU_i and δU_{i+1} , using different slope limiter procedures (Alcrudo et al., 1992). The "minmod" limiter has been followed in this study, according to which

$$\delta U_i = \text{minmod} (U_{i+1} - U_i, U_i - U_{i-1}) \quad (12)$$

$$\delta U_{i+1} = \text{minmod} (U_{i+1} - U_i, U_{i+2} - U_{i+1}) \quad (13)$$

where the minmod function is defined as

$$\min\text{mod}(a,b) = \begin{cases} a & \text{if } |a| < |b| \text{ and } ab > 0 \\ b & \text{if } |b| < |a| \text{ and } ab > 0 \\ 0 & \text{if } ab \leq 0 \end{cases} \quad (14)$$

The positive coefficient α is determined using the maximum value (for all the nodes) of the largest eigen value of the Jacobian of the system of equations. This is approximately given as

$$\alpha \geq \max \left(\frac{q_i}{h_i} + \sqrt{g h_i} \right) \quad i = 1 \text{ to } N \quad (15)$$

in which, N is the total number of grid points. All terms on the right hand side of the Eq. (9) are evaluated at the known time level n and therefore, U_i^* can be computed explicitly. The vector equation gives the predicted values of h and q at the unknown time level at any node i .

Corrector Part

The vector U at the unknown time level $n+1$ and at node i i.e. U_i^{n+1} is computed using the predicted values and the values at the time level n .

$$U_i^{n+1} = 0.5 \left[U_i^n + U_i^* - \frac{\Delta t}{\Delta x} \left(F_{i+\frac{1}{2}}^* - F_{i-\frac{1}{2}}^* \right) + \Delta t S_i^* \right] \quad (16)$$

where

$$F_{i+\frac{1}{2}}^* = \frac{1}{2} \left[F_R^* + F_L^* - \alpha (U_R^* - U_L^*) \right] \quad (17)$$

Following the recommendation of Alcrudo et al. (1992), U_R^* and U_L^* are determined from U_{i+1}^* and U_i^* using the same δU_{i+1} and δU_i as determined in the predictor step. This procedure results in better numerical stability.

In Eq. (16), only the source term in the momentum equation (the second component of the vector equation) is evaluated using the predicted values of h and q . However, the source term in the continuity equation i.e. (R-I) is evaluated using the values at the known

time level instead of the predicted values. Strictly speaking, this procedure decouples the subsurface flow computations and the surface flow computations during the computational time step Δt . However, the response of the subsurface flow to the variation in surface flow depth is much slower than the response of surface flow to changes in the rate of infiltration (Akan and Yen, 1981). Therefore, the above decoupling does not affect the results significantly. In fact, numerical experimentation showed that determination of the infiltration rate, I during the corrector step by using the predicted flow depth did not alter the results. On the other hand, the decoupling procedure resulted in significant savings of the computational time since the subsurface flow is computed only once during a time step.

3.1.1 Initial Conditions

The values of flow depth, discharge and cumulative infiltration need to be specified at all the nodes at time $t = 0$ in order to start the computations. Although dry bed conditions occur before the start of irrigation, a small uniform flow depth, h_{in} is specified at all the nodes in order to avoid the singularity problem. Correspondingly a uniform discharge (computed using the Manning equation) is also specified at all the nodes while the infiltration depth is equal to zero. The initial flow depth value is chosen such that it is as small as possible and at the same time resulted in numerically stable results.

3.1.2 Boundary Conditions

The explicit finite-difference scheme described earlier can be used to determine h and q at the unknown time level at the nodes $i = 2$ to $N-1$, where N is the total number of finite-difference grid points. The values of the variables at the upstream and the downstream ends of the domain are determined using the appropriate boundary conditions.

The discharge at the upstream end is equal to discharge supplied at the inlet point. The flow depth at the upstream end can then be determined using the negative characteristic equation (Chaudhry 1993). In the present study, a simple extrapolation procedure has been adopted to determine the upstream flow depth from the depth at the interior nodes. Numerical experimentation in the initial stages of the model development showed that the extrapolation procedure gave satisfactory results. Similar extrapolation procedure is adopted to determine h and q at the last node N .

The imposed boundary conditions vary as described below.

(i) Advance Phase $\{0 \leq t \leq t_s(n-1)\}$: At time $t = 0$, the discharge at the upstream end is increased instantaneously to a value of q_{uns} and then is held constant till the shutoff time, t_{shut} . The depth at the upstream end, h_1^{k+1} during this phase is determined using the negative characteristic equation of the governing PDEs (Chaudhry 1993) and $q_1^{k+1} = q_{uns}$. The wetting front during the advance phase is located at an intermediate point. Therefore, the flow depth and discharge at the downstream point i.e for $i = N$ are the same as the initial flow depth and discharge. Strictly speaking, the above procedure results in over specification of the downstream boundary condition. However, this does not affect the numerical results since the specified initial depths and the discharge are consistent with each other. Also, the specified initial depths are very small. It is assumed in the numerical model that the wetting front has arrived at a point i the moment the flow depth h_i^k at this point becomes greater than h_{ini} . Accordingly, the time of arrival of the wetting front at any node i , $t_s(i)$ is determined.

(ii) Storage Phase $\{t_s(n-1) \leq t \leq t_{shut}\}$: The water continues to flow into the field at the upstream end during this phase. The upstream boundary condition is the same as in the case of the advance phase. However, the treatment of downstream boundary condition is different. It is assumed that the flow stop at the downstream end i.e. discharge, $q(n)^{k+1} = q_{ini}$. The depth at the down stream end, $h(n)^{k+1}$ during this phase is determined using the positive characteristic equation of the governing PDEs (Chaudhry 1993). The infiltration depth is determined using the infiltration equation. Any other type of downstream boundary condition can easily be handled in a similar way.

(iii) Depletion and Recession $\{t \geq t_{shut}\}$: The control gate at the upstream end of the field is closed at $t = t_{shut}$ and therefore, the discharge $q(1)^{k+1}$ at this point is equal to zero for all $t \geq t_{shut}$. The flow depth $h(1)^{k+1}$ is determined using the negative characteristic equation. The depth of flow at the upstream point gradually approaches zero since the discharge is set to zero at this point. Computational problems arise in the numerical model when flow depth is zero. Therefore, the imposed upstream boundary condition in the numerical model is $q(1)^{k+1} = q_{ini}$ for all $t \geq t_{shut}$. q_{ini} is the discharge specified as the initial condition. With this boundary condition the flow depth at the upstream point gradually approaches the specified initial flow depth, h_{ini} . It is assumed in the numerical model that at the instant the flow depth $h(i)^{k+1}$ becomes less than or equal to h_{ini} . The infiltration process at node i is stopped after the arrival of the recession front. The treatment of downstream boundary condition is same as in the case of storage phase.

3.1.3 Stability Condition

The high-resolution Lax-Friedrichs scheme adopted in the present study is an explicit scheme. Therefore, the computational time step, Δt is chosen using the CFL condition.

$$C_n = \frac{\Delta t}{\Delta x} \left[\frac{q}{h} + \sqrt{g h} \right] \leq 1 \quad (18)$$

in which C_n = Courant number. Δt is chosen dynamically in the numerical model such that Eq. (18) is satisfied at all the nodes $i = 1, 2, \dots, N$.

3.2 Subsurface Flow

The one-dimensional Richards equation, Eq. 5, for subsurface flow has to be solved along with an appropriate boundary condition. In the present study, a recently developed strongly implicit finite-difference scheme (Hong et al., 1994 and Singh and Bhallamudi, 1997) for the mixed based formulation of the Richards equation is used to simulate the unsaturated subsurface flow conditions. This scheme ensures mass balance in its solution regardless of time step size and nodal spacing, and has no limitations when applied to field problems (Celia et. al, 1990). It is also easy to incorporate different types of boundary conditions in this scheme.

Numerical solution of the Richards equation is described in the following section. The subsurface flow domain is divided into a number of rectangular blocks as shown in Fig. 2. The moisture content, θ and the pressure head, ψ are specified at the centre of the block (node), while the velocities are specified at the interblock faces. The subscript j refers to the block number in the z -direction. The superscripts n and $n+1$ refer to the known and the unknown time levels, respectively. The finite-difference form of the Eq. (6) is

$$\frac{\theta_j^{n+1} - \theta_j^n}{\Delta t} + \frac{\bar{V}_{IV} - \bar{V}_{II}}{\Delta z} = 0 \quad (19)$$

where, the bar is used to denote the time-averaged value of the velocity. Δz is the nodal spacing in the z direction. The time-averaged velocities are determined by

$$\bar{V} = wV^{n+1} + (1-w)V^n \quad (20)$$

in which, w = time weighting factor. $w = 1.0$ for fully implicit scheme and it is equal to 0.5 for the Crank-Nicolson scheme.

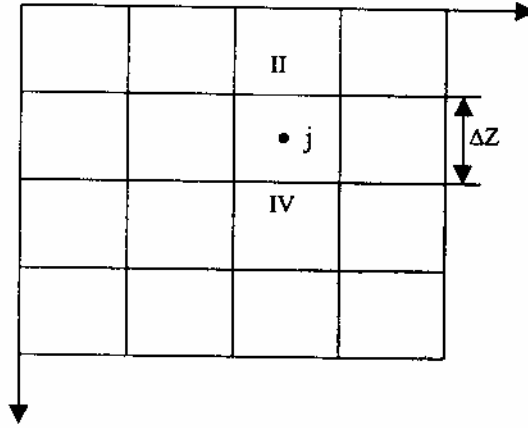


Fig. 2 Finite-Difference Grid for Subsurface Flow

The velocity at any interblock face is determined using the pressure heads at the neighbouring cell centres. For example ;

$$V_{IV} = -\frac{K_{IV} \{(\psi_{j+1} - \psi_j) - \Delta z\}}{\Delta z} \quad (21)$$

in which, K_{IV} is the unsaturated hydraulic conductivity evaluated at the interblock faces IV. Substitution of Eqs. (20), and (21) in Eq. (19) yields

$$\begin{aligned} \text{Res}_j^{n+1} = & \frac{w\Delta t}{\Delta z^2} \left[-K_{IV}^{n+1} (\psi_{j+1}^{n+1} - \psi_j^{n+1} - \Delta z) + K_{II}^{n+1} (\psi_j^{n+1} - \psi_{j-1}^{n+1} - \Delta z) \right. \\ & \left. + \theta_j^{n+1} - \left[\theta_j^n - (1-w) \frac{\Delta t}{\Delta z} (V_{IV}^n - V_{II}^n) \right] \right] = 0 \end{aligned} \quad (22)$$

The unsaturated hydraulic conductivity at an interblock face is estimated using the pressure heads at the neighbouring cell centres. Haverkamp and Vauclin (1979) state that the geometric mean is the best choice for estimating the interblock hydraulic conductivities. However, Hong et al. (1994) reported that the iterative solution of Eq. (22) fails to converge

if the above procedure is adopted for estimating the K. This is especially true for infiltration into initially very dry soils. The geometric mean is strongly weighted towards the lower value and therefore, water can not drain easily if the soil is initially dry. This result in a non-physical build up of pressure. In this study, the interblock hydraulic conductivity is estimated by the weighted arithmetic mean. For example,

$$K_{IV} = \gamma K(\psi_j) + (1 - \gamma) K(\psi_{j+1}) \quad (23)$$

in which, γ is the weight coefficient. Hong et al. (1994) suggest a value of 0.5 for γ .

Equation (22) is written for all the blocks in the flow domain and this results in a set of simultaneous algebraic equations in the unknowns $\psi(j)^{n+1}$. These simultaneous equations are highly non-linear since θ^{n+1} and K^{n+1} are non-linear functions of ψ^{n+1} . In the present study, they are solved by using the Newton-Raphson technique.

$$\text{Res}_j^{n+1,r} + \frac{\partial \text{Res}_j^{n+1,r}}{\partial \psi_m} \delta \psi_m = 0 \quad (24)$$

in which, r is the previous iteration level and $\delta \psi = (\psi^{n+1,r+1} - \psi^{n+1,r})$. Subscript m indicates the summation of the second term over all the blocks. Substituting Eq. (22) in Eq. (24) yields a linear equation in $\delta \psi$ having the following form.

$$T_j^{n+1,r} \delta \psi_{j-1} + B_j^{n+1,r} \delta \psi_{j+1} + P_j^{n+1,r} \delta \psi_j + \text{Res}_j^{n+1,r} = 0 \quad (25)$$

in which, T , B , and P are the elements of the Jacobian of the system of equations, Eq. (22). Equations for evaluating these are presented in Appendix-I. Equation (25) when written for all the blocks in the domain constitutes a matrix equation .

$$A^{n+1,r} \delta \psi = -\text{Res}_j^{n+1,r} \quad (26)$$

in which, the coefficient matrix A is banded. Equation (26) is solved in the present study using an efficient NAG LIBRARY, subroutine TRIDOG.

For convergence in iteration of Eq. (24), it is required that

$$|Res_j^{n+1,r}| < \varepsilon \quad (27)$$

in which, ε = water content convergence tolerance. Equation (27) practically represents the principle of mass conservation because usually a very small value of ε is imposed.

3.2.1 Initial Conditions

The values of suction head, moisture content and unsaturated hydraulic conductivity need to be specified at all the nodes at time $t = 0$ in order to start the computations. A very small value of moisture content, θ_{ini} is specified at all the nodes as initial conditions. Correspondingly a suction head and unsaturated hydraulic conductivity (computed using the characteristic equation) is also specified at all the nodes.

3.2.2 Boundary Conditions

(i) *Flux-Type Boundary Conditions*: In the present scheme, the grid is arranged in such a manner that the boundaries of the flow domain coincide with the top cell face. Therefore, flux or velocity-type boundary condition can be incorporated in a natural way in Eq. (19).

(ii) *Pressure Head-Type Boundary condition*: Referring Fig. 3, let ψ_b be the imposed pressure head at the ground surface of the flow domain. This pressure head ψ_b is used along with the values of ψ_1 , pressure head at the first node and ψ_2 pressure head at the second node in the z-direction to determine the flux at the ground surface as given below

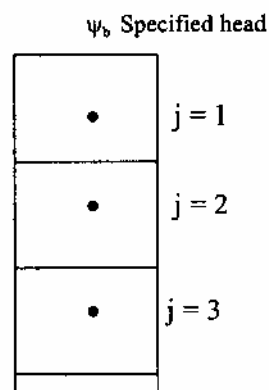


Fig. 3 Definition Sketch of Pressure Head type Boundary Condition

$$V_z|_{z=0} = -K(\psi_b) \left\{ \frac{(-8\psi_b + 9\psi_1 - \psi_2)}{3\Delta z} - 1 \right\} \quad (28)$$

Second-order forward finite-difference analog is used to determine the above Eq. (28). Equation (22) and equations for the coefficients T, B & P are appropriately changed to include the boundary conditions before the matrix $A^{n+1,r}$ in Eq.(26) is formed.

3.3 Calculation of Evapotranspiration (Sink Term)

The sink term can be computed using potential evapotranspiration, crop coefficient, soil moisture status and variation of root density along depth. Evapotranspiration is related to pan evaporation by a constant K called consumptive use coefficient. The formula for K is given as

$$E_{vpt} = K E_p \quad (29)$$

in which, E_{vpt} is the evapotranspiration; E_p is the pan evaporation; and K is the consumptive use coefficient, which depends upon the type of crops and stages of crop growth. Hargreaves has given the values of K for different crops and at different stages of crop growth (Garg, 1986). The pan evaporation can be experimentally determined by direct measurement of the quantity of water evaporated from the class A pan. The pan evaporation can also be determined by using the Christiansen formula, which has been introduced in this source code, only input data for this equation has to give. The actual evapotranspiration can be computed based on the moisture content and the distribution of the root in the root zone of the soil.

3.3.1 Variation of Evapotranspiration with Soil Moisture

The actual evapotranspiration variation based on the moisture content of the soil is given as (Fig. 4)

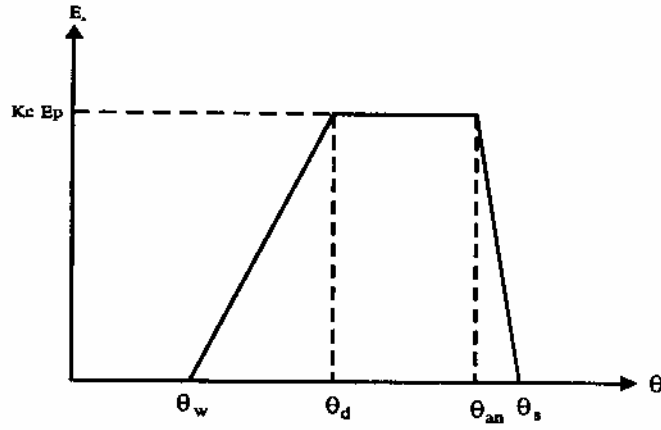


Fig.4 : Plant Root Uptake Function E_a with Soil Moisture.

$$E_a(0,t) = \begin{cases} K E_P \left(\frac{\theta - \theta_w}{\theta_d - \theta_w} \right) & \text{For } -15800 \text{ cm} \leq \psi \leq -400 \text{ cm} \\ K E_P & \text{For } -400 \text{ cm} \leq \psi \leq -50 \text{ cm} \\ K E_P \left(\frac{\theta_s - \theta}{\theta_s - \theta_{an}} \right) & \text{For } -50 \text{ cm} \leq \psi \leq 0 \text{ cm} \end{cases} \quad (30)$$

where, $E_a(0,t)$ actual evaporation (cm); K is the consumptive use coefficient (defined as the ratio of evapotranspiration to Pan evaporation, E_p), and is different for different crops and crop growth; θ is the moisture content; θ_w is the moisture content at wilting point (at $\psi = -15800$ cm); θ_d is the moisture content at $\psi = -400$ cm; θ_{an} is the moisture content at anaerobiosis point (at $\psi = -50$ cm); θ_s is the saturated moisture content.

The variation of actual evapotranspiration along depth in root zone depth, d , is as follows (Michael, 1978):

$$S_i(z,t) = \begin{cases} 0.4 E_a(0,t) & \text{For } 0 \leq z \leq \frac{d}{4} \\ 0.3 E_a(0,t) & \text{For } \frac{d}{4} \leq z \leq \frac{d}{2} \\ 0.2 E_a(0,t) & \text{For } \frac{d}{2} \leq z \leq \frac{3d}{4} \\ 0.1 E_a(0,t) & \text{For } \frac{3d}{4} \leq z \leq d \end{cases} \quad (31)$$

where, d = root zone depth; z is the actual depth of the particular node

This sink term is used in the subsurface flow equation and solved for the computation of the moisture content along depth.

3.4 Surface and Subsurface Flow Interaction

Surface and subsurface flow components are interrelated by a common pressure head and the infiltration at the ground surface. The surface flow depth determines the top boundary condition for the subsurface flow. In turn, the infiltration term in the surface flow equation is controlled by the subsurface flow conditions. The following procedure is adopted for simulating the interaction between the surface and the subsurface flow components.

1. Subsurface flow solution at time level n is used to determine the infiltration rate at the ground surface.
2. Surface flow equations are now solved using the infiltration rate from step 1 to determine q and h at the unknown time level $n+1$.
3. The surface flow depth at the time level $n+1$ is used as the top boundary condition and the subsurface flow equations are solved. This gives the moisture content, θ and suction, ψ distribution in the subsurface at time level $n+1$.
4. Steps 1-3 are repeated up to the required time level.

3.4.1 Boundary Conditions

For subsurface flow resulting from irrigation infiltration, the top boundary condition changes with time. During the initial stages of the irrigation, there is ponding and the head type of boundary condition ($\psi_b(x) = h(x) =$ water flow depth at that point) is applied. As time progresses, the water gets infiltrated into the ground, which starts decreasing of flow depth at the surface. When all water gets infiltrated into the soil then the pressure head at the surface is computed if the relative humidity (f) and the temperature of the air (T) as a function of time are known. It may be assumed that the pressure head at the soil surface is at equilibrium with the atmosphere, then $\psi(0,t)$ from the thermodynamic relationship (Edlefsen and Anderson, 1943) is given as:

$$\Psi(0,t) = \frac{R T(t)}{M g} \ln [f(t)] \quad (32)$$

where, $\psi(0,t) = \psi_0$ is the pressure head at the surface (bar); R is the universal gas constant (8.314×10^7 erg/mole/K), T(t) is the absolute temperature (K), g is acceleration due to gravity (980.665 cm/s^2), M is the molecular weight of water (18 gm/mole), f(t) is the relative humidity of the air (fraction) and ψ is in bars (1 bar = 1019.80 cm of water).

The ψ values at the bottom boundary are obtained using a simple extrapolation from the interior points if the water table is deep. If the water table is at the bottom then the phreatic surface acts as bottom boundary of the system and the pressure head is equal to zero.

3.4.2 Soil Moisture Characteristics

The following typical functional relations, as reported by Haverkamp et al. (1977), for characterizing the hydraulic properties of a soil, can be used.

$$K(\Psi) = K_s \frac{A}{A + |\Psi|^m} \quad (33)$$

and

$$\theta(\Psi) = \theta_r + \frac{B(\theta_s - \theta_r)}{B + |\Psi|^n} \quad (34)$$

where, K(ψ) is the unsaturated hydraulic conductivity (cm/hr); K_s is the saturated hydraulic conductivity (cm/hr); $\theta(\psi)$ is the moisture content; θ_s is the saturated moisture content and θ_r is the residual moisture content; A, B, m and n are the constants.

4.0 RESULTS AND DISCUSSION

4.1 Simulation of Hypothetical Case Study

A numerical simulation was carried out using the present model to demonstrate the applicability of the model. In the early stage of the model development, only the subsurface flow equation with the sink term has been solved. The developed model has been used to simulate the different scenarios of irrigation water application, such as constant head (for paddy), and variable heads (for sugar cane) at the ground surface and with and without sink term in the Richards equation. Later, the model has been developed considering all the processes of the cropped, such as surface flow, subsurface flow, evapotranspiration from crop and return flow below the root zone. The applicability of both the models are demonstrated below.

4.1.1 Subsurface Flow with Sink

For this purpose, a hypothetical cropped field has been considered. The length of the field and depth of the unsaturated zone are 10 m and 60 cm respectively. The input parameters considered are depth of irrigation water = 10 cm; saturated hydraulic conductivity, $K_s = 0.8$ cm/hr; saturated moisture content, $\theta_s = 0.4$; residual moisture content, $\theta_r = 0.08$. The constants for the characteristic relationship are as follows, $A = 2.014$; $m = 1.234$; $B = 20.73$; and $n = 0.411$. As evapotranspiration is calculated on the basis of pan evaporation, its value has to give as input. Pan evaporation is taken as 3 mm per days. The initial condition for the subsurface is specified as the initial moisture content, $\theta_{in} = 0.1$. Though, two methods (Pan evaporation and Christiansen formula) of evaporation have been considered for the computation of evapotranspiration from the crop, only one method (pan evaporation) is demonstrated. The evapotranspiration has been calculated based on the pan evaporation method.

(i) Variable Head with Sink Term

Variable head means a certain depth of irrigation water is applied in the field and let the water infiltrate into the ground. As time progress all water infiltrates into the ground and the moisture content below the ground advances in down ward direction accordingly. When depth of water at the surface is zero then there is no infiltration, but there is a upward flux due to the evapotranspiration from crop, which causes the recession of the moisture content towards the down ward direction. As recession progresses the moisture content reaches to the wilting point and crops are unable to take water from the soil and yield is affected. To

overcome with this stage next irrigation is required. In the present study, the model is used to simulate the irrigation scheduling up to the 14 days. Two irrigation cycles have been applied. The movement of the moisture content at a section along the depth is presented at different time for advance and recession phases. The results obtained from the present model for the advancement of the moisture front (wetting front) below the ground have been presented in Fig. 5. This figure shows the moisture profiles (wetting front) along the depth below ground at different time level i.e. at 0 hr, 3 hrs, 5 hrs and 10 hrs after application of water at the surface. Figure shows that as time progresses the moisture content near the surface increases and finally gets saturated at time, $t = 10$ hr. It can be seen from figure that the saturation is up to the depth of about 10-cm and moisture increases below this depth from the initial values along depth and it moves down. At time, $t = 10$ hrs, all water at surface gets infiltrated in to the ground. Since there is a sink term to consider the evapotranspiration from the crop, the moisture in root zone starts decreasing and therefore there is a recession in the moisture front near the ground surface. The recession phase has been shown in Fig. 6. The moisture profiles (wetting fronts) at time, $t=10$ hrs, 18 hrs, 2 days and 7 days have been presented in this figure. It can be seen that as time progresses, some moisture moves down ward and some moisture consumed by crops through the evapotranspiration. It means the moisture decreases in the upper layer and increases in the lower layer. It can also be seen that at time, $t = 7$ days, the moisture near the surface has decreased nearly up to the wilting point, which shows the time of next irrigation.

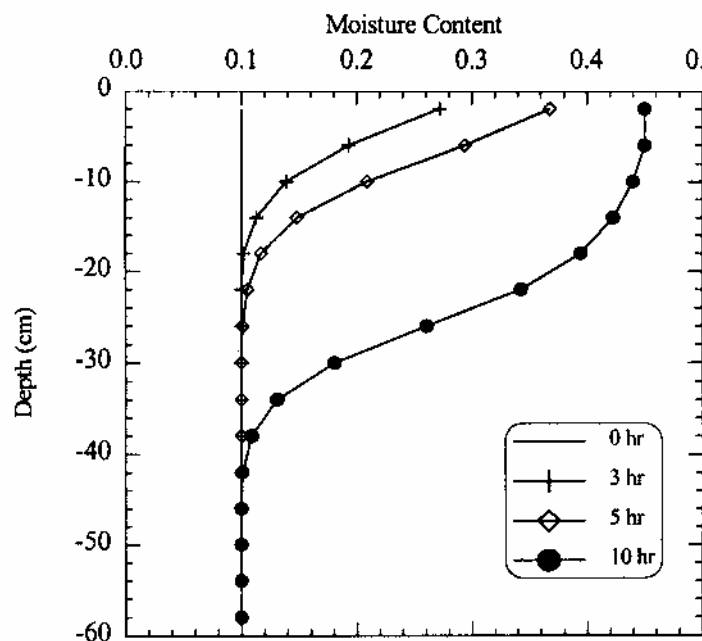


Fig. 5 Movement of Moisture Front below Ground Surface in Advance Phase

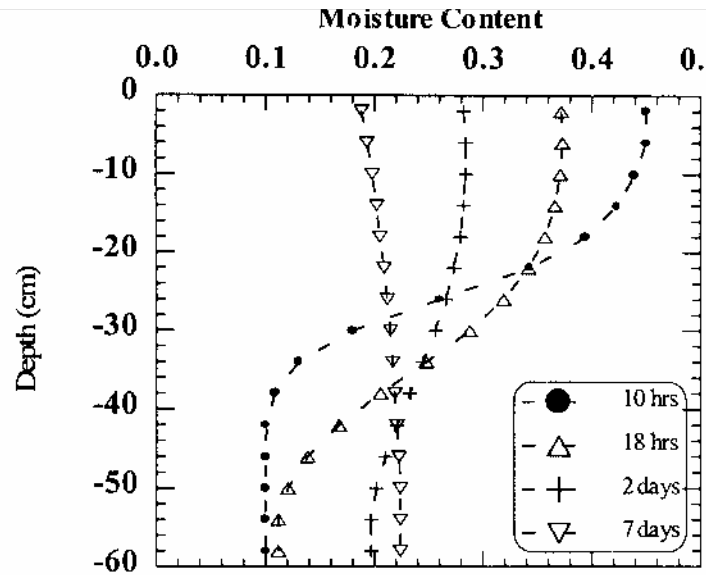


Fig. 6 Movement of Moisture Front below Ground Surface in Recession Phase

Next irrigation of depth 10 cm has been applied at the surface after 7 days. Figure 7 presents the advancement and recession of the moisture profiles (wetting front) for second irrigation i.e. at time, $t = 7$ days, 7 days 1 hr, 7 days 8 hrs, 8 days and 14 days. The solid line represents the advancement of the wetting fronts and dashed lines represents the recession of the wetting fronts. At time, $t = 7$ day moisture profile below the ground is at minimum moisture and as time progresses again it moves down ward. At time $t = 7$ days 8 hrs soil near the surface and up to depth of 25 cm below ground is completely saturated and all water above the surface gets infiltrated into the ground. After 7 day and 8 hrs wetting front under the ground starts recession. Again it can be seen from Fig (8) that as time progresses some part of moisture from the root zone consumed by crops and some moves down ward. At time $t = 14$ days the moisture profile is at the minimum moisture content and it shows the time of next irrigation. It can be seen that at time, $t = 7$ days the moisture goes below 0.2 and at time, $t = 14$ days it is more than 0.2. This is due to the initially dry soil in root zone more moisture consumed in dry case but initial moisture status at 7 days is more than at initial time.

The sink term computed at different time at a section has been presented in Fig. (8), (9) and (10) for advance phase, recession phase and for the next irrigation, respectively. It can be seen from Fig. (8), that for initially dry soil in root zone there is no evapotranspiration and as time progresses the moisture in root zone increases and evapotranspiration also increases near the surface. It is clear from Fig. (11) that near the surface soil is completely saturated and therefore, there is more evapotranspiration from this layer of soil (Fig. (8) and (9)). Figure (9)

shows that after time, $t = 18$ hrs moisture near surface is decreasing and hence the evapotranspiration in this layer is also decreasing. As moisture is minimum at time, $t = 7$ days the rate of evapotranspiration is minimum. Similar patterns of the evapotranspiration have been shown in Fig. (10) for advancement and recession phases of the wetting fronts.

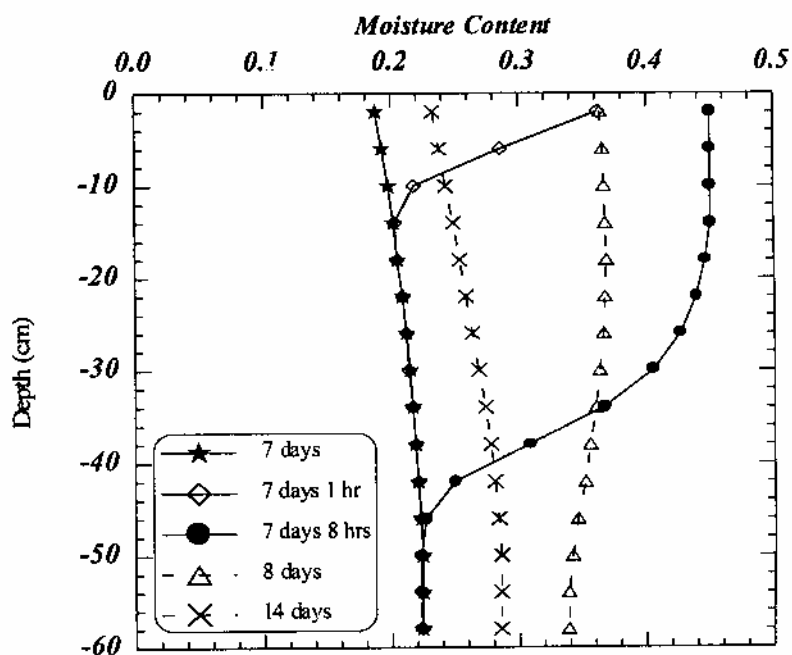


Fig. 7 Moisture Content Profile in next irrigation (Advance & Recession)

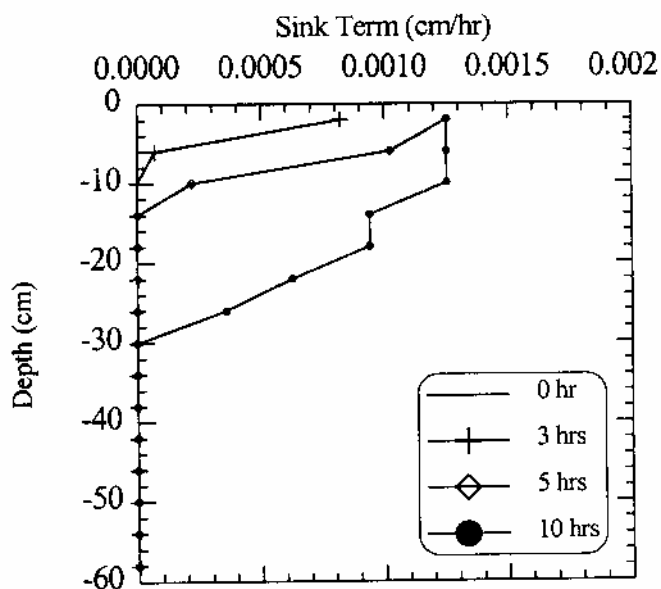


Fig. 8 Variation of Sink Term along depth for Advance Phase

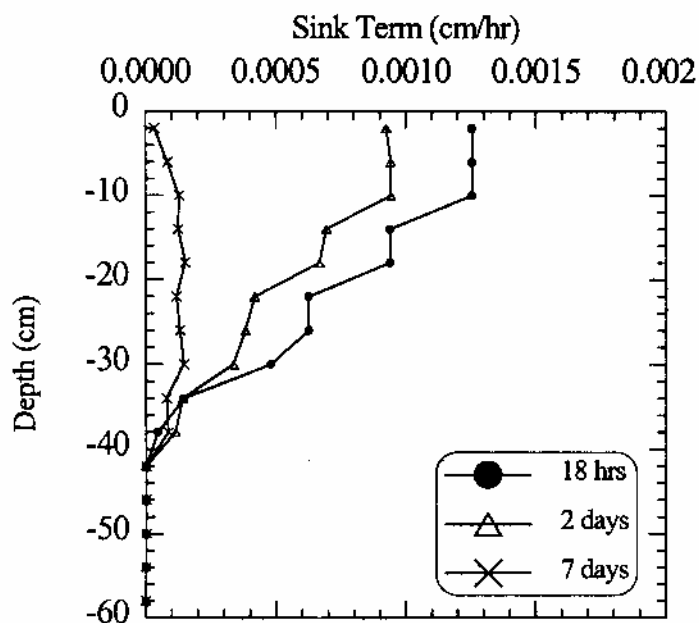


Fig. 9 Variation of Sink Term along depth for Recession Phase

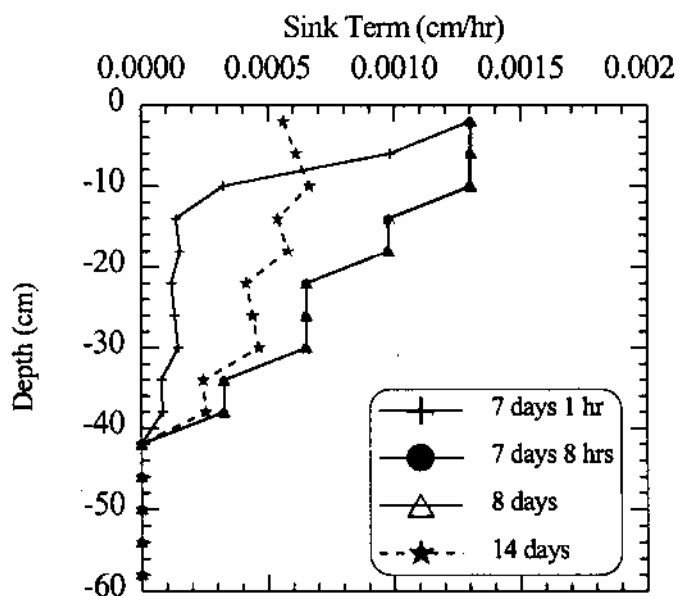


Fig. 10 Sink Term after second Irrigation along depth for Advance & Recession

It can be seen from Fig. (10) that at and after time $t = 7$ days and 8 hrs, there is maximum rate of evapotranspiration from the crop. It means when the moisture is in between the field capacity and near saturation, there is maximum evapotranspiration from the crop due

to the easily and readily available of water in root zone. As moisture decreases below the field capacity there is a decrease in evapotranspiration.

(ii) Variable Head without Sink Term

The present model is used to simulate the case of variable head and without sink term. Without sink term means there is no evapotranspiration from the crop i.e. field without crops. This case has been simulated with same input data as with sink term except data, which are required for evapotranspiration. The results have been presented in Fig. (11) and (12) along with the results with the sink term. Figure (11) shows the advance phase of the moisture and Fig. (12) shows the recession phase of the moisture. In these figures solid lines show the results with sink term where as the dashed lines show the results without sink term. From Fig. (11) it can be seen that in initial stage of the crop growth, there is no effect of sink term on the moisture movement because of the little amount of the evapotranspiration from less root density. As time progresses, the crop growth increases and root density increases and that takes more water, so there is more evapotranspiration from the crop.

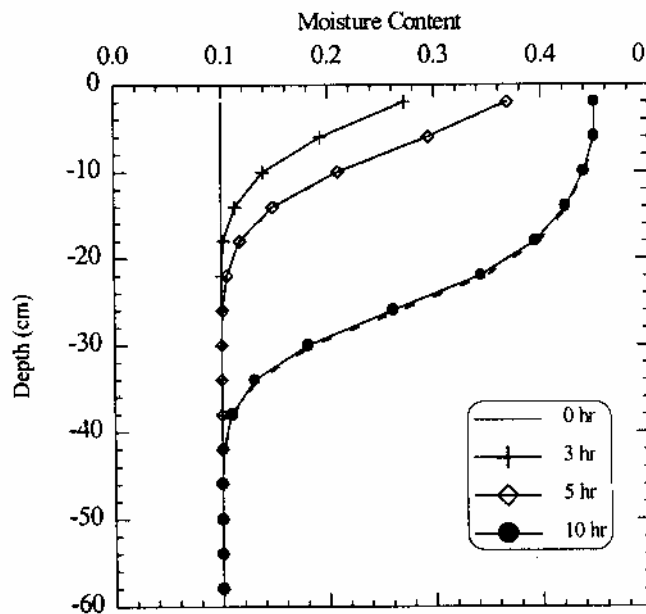


Fig. 11 Moisture Profiles with & without Sink Term at different time along depth (Advance)

In the initial time of the crop growth there is no variation the moisture profiles but as time progresses the root of the crop increases and it consumes more moisture and there is effect of evapotranspiration on moisture profiles in the root zone. It can be seen from Fig. (12) that, at time, $t = 18$ hrs and onward results obtained without sink term shows more moisture than the results with sink term as they are lagging. It is more clear for time, $t = 2$ days and 7 days. Though the results have been obtained up to 14 days it is not shown after 7 days. It was found that sink term effect was more.

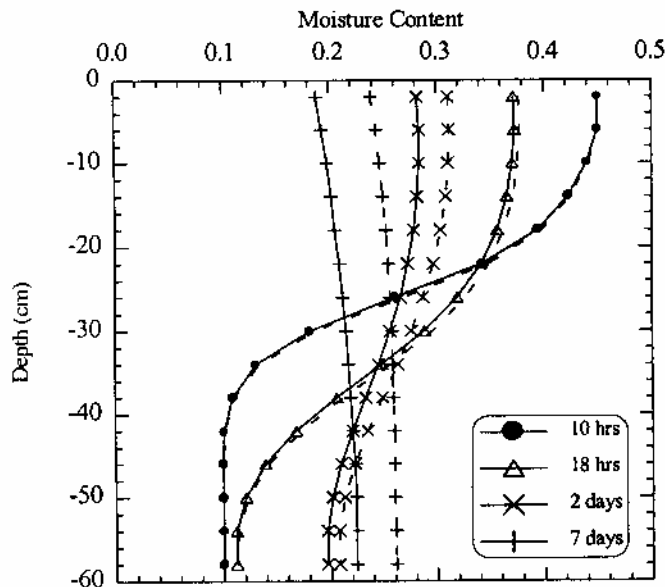


Fig. 12 Moisture Profiles with & without Sink Term at different time along depth (Recession)

(iii) Constant Head with Sink Term

A case of constant head with sink term has also been simulated for the paddy crop. In paddy crop, always there is standing water in the field and there is evapotranspiration from the crop. For paddy crops the root zone depth is less than the sugar cane, it is taken as 20 cm below the ground. In this model, the input data are same as applied for the sugar cane except the root zone depth, which is taken as 20 cm. As the time progresses, the soil near the surface gets saturated and saturation front moves down. After certain time whole root zone depth is completely saturated due to the standing water at the surface. Figure (13) presents the moisture profile along the depth at different time, $t = 1$ hr, 2 hrs, 5 hrs, 6 hrs, 12 hrs, 18 hrs and 20 hrs. It can be seen from Fig. (13) that at time, $t = 6$ hrs, soil near the ground gets saturated and it moves down. At time, $t = 12$ hrs the soil is completely saturated up to the

depth of 22 cm and the moisture profile reached up to 40 cm. It is found that at time, $t = 20$ hrs whole root zone depth is completely saturated and water flows at the rate of saturated hydraulic conductivity.

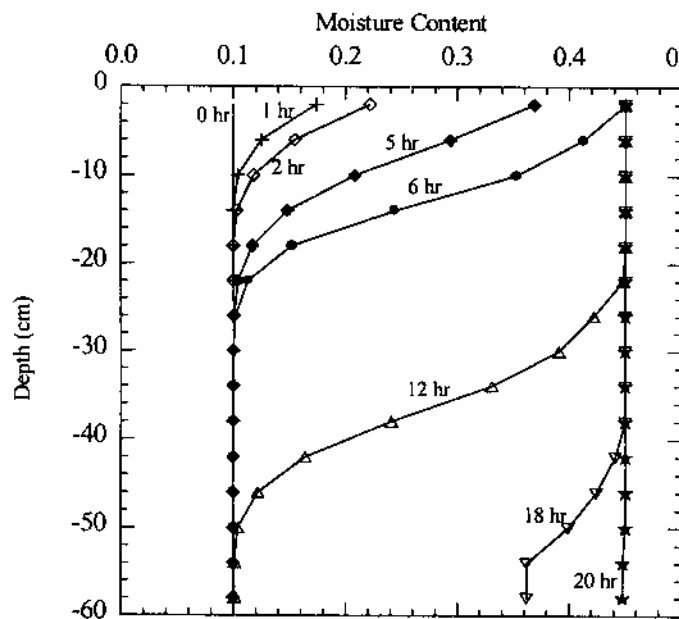


Fig. 13 Moisture Profiles with Sink Term for Constant Head at different time along depth (Advance)

Figure (14) presents the variation of the sink term (evapotranspiration from the paddy crops). In this figure, the distribution of sink term along the depth have been presented at time, $t = 3$ hrs, 5 hrs, and 8 hrs. Figure shows that as time progresses, rate of evapotranspiration increases and reached maximum rate at time, $t = 8$ hrs and transpired moisture with the constant rate. Since the rate of evapotranspiration is constant after 8 hrs so no more distribution has been shown. The return flow in the case is more due to complete saturation exists for more time.

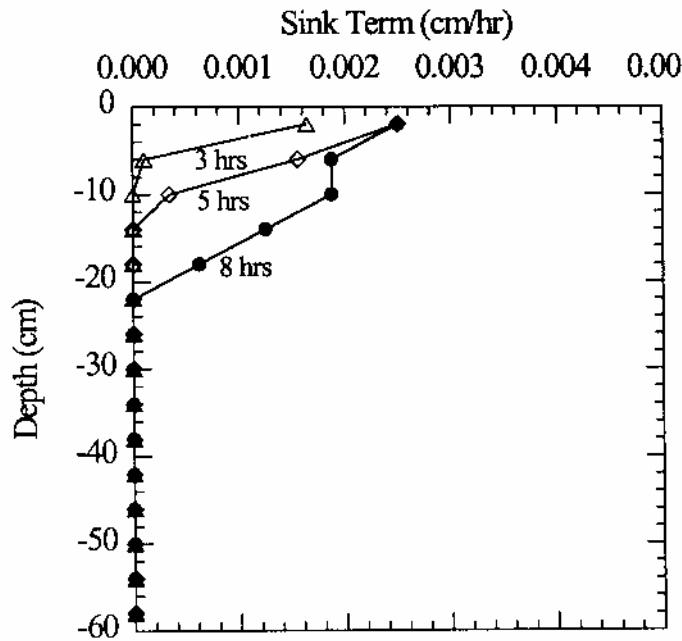


Fig. 14 Variation of Sink Term (evapotranspiration) along the Depth and Time

4.1.2 Surface and Subsurface Flow with Sink

In this model, surface flow, and subsurface flow equations along with the sink term, to consider the evapotranspiration from the crops, have been solved. Surface flow has been solved to show the advancement of the surface water profile at different time along the length of the field. It means how much time water takes to reach the down stream end. For this purpose, a field of 25 m long has been considered. The input parameters for surface flow component are slope of the field, $S_o = 0.0001$, and the Manning roughness, $n = 0.035$, irrigation water supplied at the upstream end, $q_{uns} = 0.003 \text{ m}^3/\text{s}$ per unit width, the time of cut off the irrigation supply, $t_{shut} = 1200 \text{ sec}$, and space step, $\Delta x = 0.5 \text{ m}$. The maximum time of simulation is 10 hrs to show the applicability of the model. The input parameters for subsurface flow components are same as taken for the simulation of subsurface flow component only.

The results obtained from the present model have been presented to show the time of wave arrival at particular node i , it means what is the time taken by the water to reach a particular length of the field. It will give the time taken by water to reach the downstream end. Figure (15) shows the time of water arrival at different position along the length of the

field. This is the time when the surface water depth is greater than initial flow depth, h_{ini} at particular section of the length. It can be seen from Fig. (15) that the time of water arrival is more or less linear after the length of 5 m. From this figure it can also be seen that water reached to down stream end in 120 sec. Though, the length of the field is small, the time of water arrival depends on the slope of the field, Manning roughness of the bed, sub soil characteristic and the irrigation water applied at the upstream end. Since all the parameters are hypothetical, so this figure can be different for different set of data or can vary with the exact data of the field.

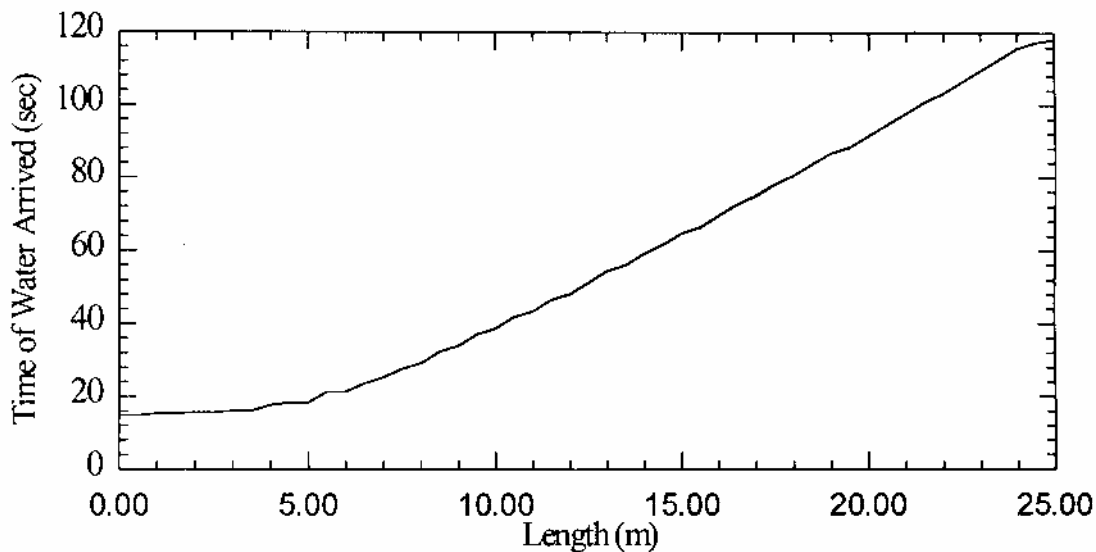


Fig. 15 Time of Water Arrival along the Length of the Field

The results obtained from the present model are presented for the advancement of the wave front (surface water depth) and the position of the wetting front along the length at different time. The wetting front is considered as the moisture content, which is slightly greater than the field capacity. Figure (16) presents the position of surface water depth and wetting front along the length at different time. The solid lines represents position of the surface water depth and dashed lines represents the position of the wetting front below ground. These positions have been shown at time, $t = 50$ sec, 100 sec, 200 sec, 10 min. and 20 min. It is clear from the figure that at time, $t = 50$ sec water has arrived at 11 m length and at 100 sec the water is arrived up to 20 m length. It can also be seen from the Fig. 15 that the water arrival time for 20 m length is 100 sec. At time 200 sec the whole length have the water depth of approximately 0.025 m and as time progresses water depth increases and it is 0.14 m at time 20 min, which is maximum. Since the 20 min is the shut off time so, after this time

water starts decreasing and the phase is called recession phase. It can also be seen from Fig (16) that the wetting front below the ground has not moves much in initial stage. It means less amount of water has been infiltrated below the ground up to this time. The recession phase has been shown in Fig. (17).

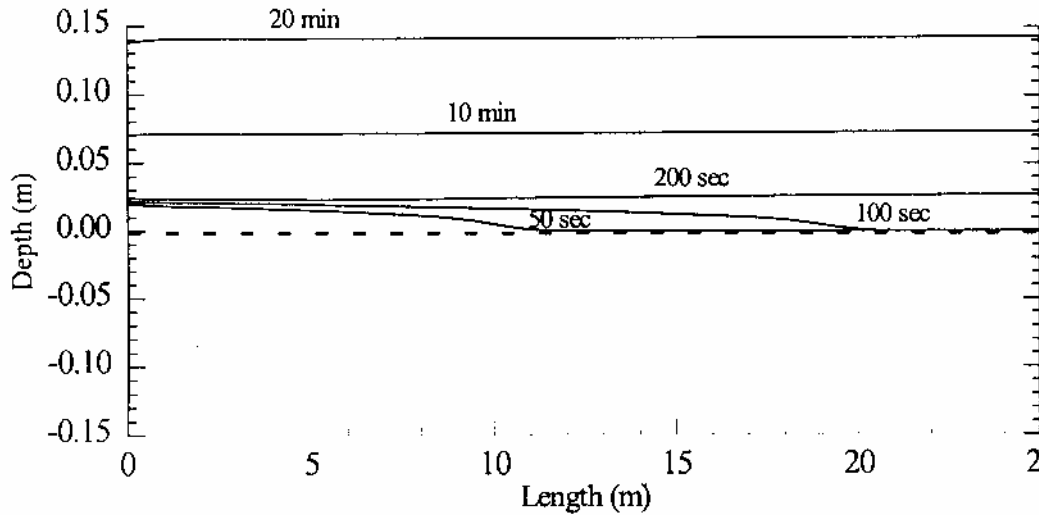


Fig. 16 Surface Water Depth and Wetting Front at different time (Advance Phase)

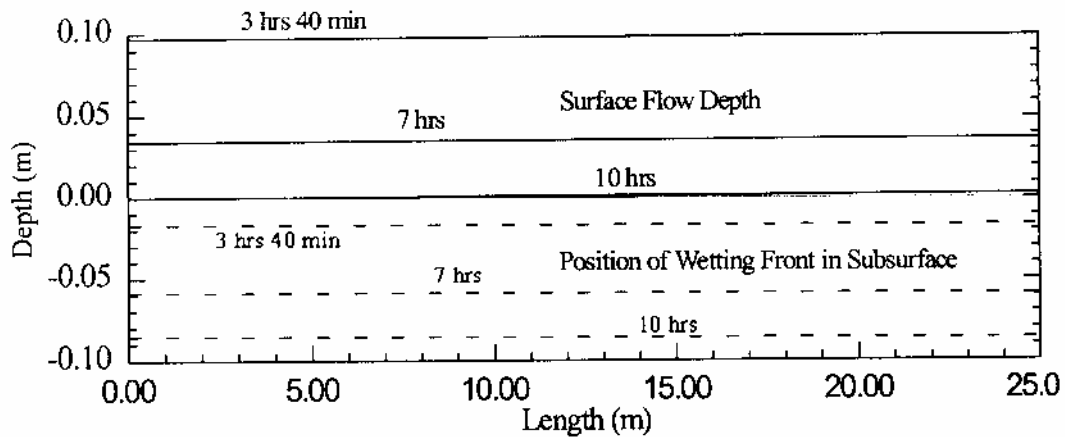


Fig. 17 Position of the Surface Water Depth and Wetting Front at different Time (Recession Phase)

In this figure, again solid lines represent the surface water depth and dashed lines represents the wetting front at different time. Figure (17) shows that at time 3 hrs and 40 min the surface water depth decreased up to the depth of 0.1 m at upstream end. There is slightly

more depth of water at the down stream end, this may be due to the slope of the field. The soil moisture front has arrived up to the depth of 0.02 m. As time progresses the surface water depth decreases and simultaneously the wetting front moves downward. It can be seen that at time 10 hrs, all surface water has infiltrated into the ground and wetting front has moved down the maximum depth.

The movement of the moisture content has been shown in Fig. (18) at time 50 sec, 20 min, 2 hrs, 4 hrs 40 min, 6 hrs 40 min and 9 hrs 30 min. It can be seen that at time 6 hrs 40 min the subsoil near the ground surface has got just saturated and before this the moisture content were less for all the depth. The wetting front is considered as the moisture, which is more than the field capacity, but this figure shows the exact moisture content along the depth at different time. The saturation front has reached up to the depth of 10 cm at time 9 hrs 30 min.

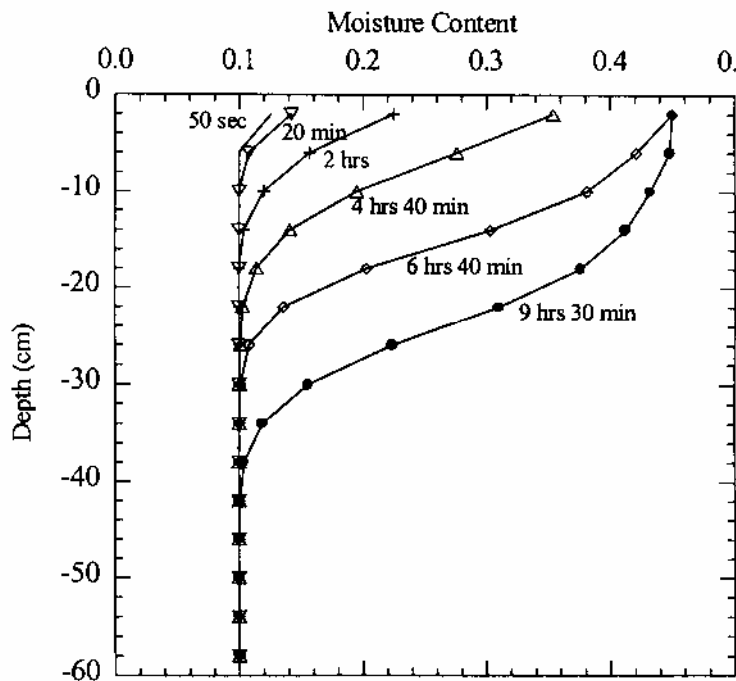


Fig. 18 Movement of Moisture Content along depth at different Time

Figure (19) presents the variation of the sink term (evapotranspiration from the crop) along the depth and at time 2 hrs, 4 hrs 40 min, 6 hrs 40 min and 9 hrs 30 min. In initial stage of crop growth, there is low root density in the root zone. It results less amount of evapotranspiration from the crop. But as time progresses, the root density increases and

therefore the evapotranspiration from crop also increases and it is maximum at time 9 hrs 30 min.

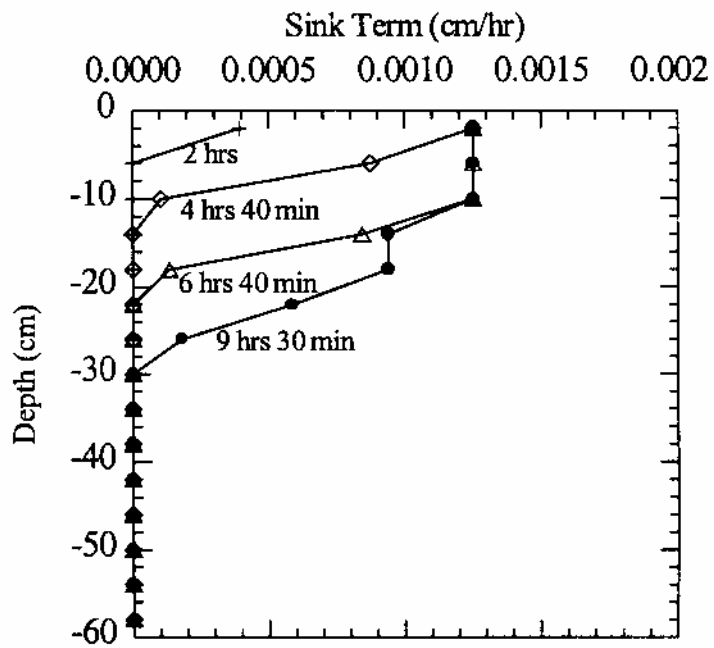


Fig. 19 Variation of Sink term along Depth at different Time

5.0 CONCLUSION

A model has been developed considering one-dimensional St. Venant equations for surface flow component and one-dimensional Richards equation for subsurface flow component along with the evapotranspiration from the crop as the sink term. The sink term is calculated considering the crop coefficient, potential evaporation, moisture content in the root zone and the distribution of the root density along the root zone depth. The surface flow equations are solved using second order accurate, explicit, essentially-non-oscillating (ENO) finite difference scheme. The strongly implicit procedure is used to solve the subsurface flow equation. Two models have been developed. First model is for subsurface flow component only with the sink term. Second model is for the complete processes, such as surface flow and subsurface flow components along with the sink term for evapotranspiration from the crop. The present model is used to simulate the various scenarios of the irrigation for different crops.

Since the main objective of this study was the development of the model for surface runoff, infiltration and evapotranspiration from the cropped field, the simulation time has been taken only up to 10 hrs to show the applicability of the model. Now the model is ready and it can be applied to the field after verification with the field data.

The numerical experimentation shows that to estimate the irrigation return flow from cropped field by soil moisture modelling, only subsurface flow component with the evapotranspiration term is sufficient. If the surface flow component is added, it shows only the advancement of the water along the length of the field and it takes only 200 sec. There is less infiltration within this time, therefore, this component can be avoided, while simulating the cropped field. However, it very important component for overland flow.

REFERENCES

- Akan, A.O., & Yen, B.C.,(1981), "Mathematical model of shallow water flow over porous media", *J. of Hydraulic Division*, 107(HY4), 479-494.
- Alcrudo F., Garcia-Navarro P., & Saviron, J.M., (1992), "Flux difference splitting for 1D open channel flow equations", *Int. J. Numerical Methods in Fluids*, 14, 1009-1018.
- Allen, M.B., & Murphy, C.L., (1986), "A finite-element collocation method for variably saturated flow in two space dimensions", *Water Resources Research*, 22(11), 1537-1542.
- Bassett, D.L., (1972), "Mathematical model of water advance in border irrigation," *Transaction, ASAE*, 15(5), 992-995.
- Bassett, D.L., and Fitzsimmons, D.W., (1976), "Simulating overland flow in border irrigation," *Transaction, ASAE*, 19(4), 666-671.
- Bautista, E., and Wallender, W.W., (1992), "Hydrodynamic furrow irrigation model with specified space steps," *J. Irrig. Drain. Engg.*, ASCE, 118(3), 450-465.
- Bautista, E., and Wallender, W.W., (1993), "Identification of furrow intake parameters from advance times and rates," *J. Irrig. Drain. Engg.*, ASCE, 119(2), 295-311.
- Celia, M.A., Bouloutas, E.F., & Zarba, R.L., (1990), "A general mass-conservative numerical solution for the unsaturated flow equation", *Water Resources Research*, 26(7), 1483-1496.
- Chandra, Satish, (1979), "The estimation of ground water recharge", *J. of Hydrology*, 41, 345-361.
- Chaudhry, M.H., (1993), "Open-channel flow", Prentice-Hall, Englewood Cliffs, New Jersey.
- Edlefsen, N. E. and Anderson, A. B. C. (1943), "Thermodynamics of Soil Moisture", *Hilgardia*, 15, 31-298.
- Freeze, R.A. & Cherry, J.A., (1979), "Ground Water", Prentice-Hall, Englewood Cliffs, New Jersey.
- Garg, S. K. (1996), "Irrigation Engineering and Hydraulic Structures", Khanna Publishers, New Delhi.
- Haverkamp, R., and Vauclin, M., (1979), "A note on estimating finite-difference interblock hydraulic conductivity values for transient unsaturated flow problems", *Water Resources Research*, 15(1), 181-187.

- Haverkamp, R., Vauclin, M., Touma, J., Wierenga, P. J. and Vachaud, G. (1977), "A Comparison of Numerical Simulation Models for One-Dimensional Infiltration", *Soil Sci. Soc. Am. J.*, 41, 285-294.
- Hills, R. G., Porro, I., Hudson, D. B., and Wierenga, P. J., (1989), "Modelling one dimensional infiltration into very dry soil 1. Model development and evaluation", *Water Resources Research*, 25(6), 1259-1269.
- Hong, L. D., Akiyama, J., and Ura M., (1994), "Efficient mass-conservative numerical solution for the two-dimensional unsaturated flow equation", *J. of Hydroscience and Hydraulic Engineering*, 11(2), 1-18.
- Katopodes, N.D., and Strelkoff, T., (1977), "Hydrodynamics of border irrigation-complete model," *J. Irrig. Drain. Div.*, ASCE, 103(IR3), 309-323.
- Kincaid, D.C., Heermann, D.F., and Kruse, E.G., (1972), "Hydrodynamics of border irrigation advance," *Transaction*, ASAE, 15(4), 674-680.
- Michael, A. M., (1978), "Irrigation Theory and Practice", Vikas Publishing House Pvt. Ltd., New Delhi.
- Miller, D.E., (1967), "Available water in soil as influenced by extraction of soil water by plants", *J. Agronomy*, 59(5), 420-423.
- Mohan Rao, K. M., Kashyap, D. and Satish Chandra, (1990), "Relative performance of a soil moisture accounting model in estimating return flow", *J. of Hydrology*, 115, 231-241.
- Nujic, M., (1995), "Efficient implementation of non-oscillatory schemes for the computation of free-surface flows", *J. Hydraulic Research*, IAHR, 33(1), 101-111.
- Parlange, J.Y., Haverkamp, R., and Touma, J., (1985), "Infiltration under ponded condition: 1. optimal analytical solution and comparison with experimental observation," *Soil Science*, 139(4), 305-311.
- Playan, E., Walker, W.R., and Merkle, G.P., (1994), "Two-dimensional simulation of basin irrigation I:Theory," *J. Irrig. Drain. Engg.*, ASCE, 120(5), 837-855.
- Rawls, W.J., and Brakensick, D.L., (1988), "Estimating soil hydraulic properties", J. Morel Seytoux(ed.), *Unsaturated Flow in Hydrologic Modelling*, Riedel, 275-300.
- Sakkas, J.G. and Strelkoff, T., (1974), "Hydrodynamics of surface irrigation-Advance phase," *J. Irrig. Drain. Div.*, ASCE, 100(IR1), 31-48.
- Schmitz, G., Haverkamp, R., and Palacios, O., (1985), "A coupled surface-subsurface model for shallow water flow over initially dry soil," *Proc., 21st Congress IAHR, International Association for Hydraulic Research*, 1, 23-30.

Singh, V. and Bhallamudi, S. M., (1996), "Complete Hydrodynamic Border-Strip Irrigation Model", *Journal of Irrigation and Drainage Engineering*, ASCE, 122(4), 189-197.

Singh, V. and Bhallamudi, S. M., (1998) "Conjunctive Surface Subsurface Modeling of Overland Flow," *Advances in Water Resources*, 21(7), pp. 567-579.

Wallender, W.W., and Rayej, M., (1990), "Shooting method for Saint Venant equations for furrow irrigation," *J. Irrig. Drain. Engg.*, ASCE, 116(1), 114-122.

APPENDIX - I

Elements of the Banded Matrix

$$W_{i,j}^{n+1,r} = \frac{w\Delta t}{\Delta x^2} \left\{ -K_I^{n+1,r} + \frac{D_{i-1,j}^{n+1,r}}{2} (\psi_{i,j}^{n+1,r} - \psi_{i-1,j}^{n+1,r}) \right\} \quad (I-1)$$

$$E_{i,j}^{n+1,r} = \frac{w\Delta t}{\Delta x^2} \left\{ -K_{III}^{n+1,r} - \frac{D_{i-1,j}^{n+1,r}}{2} (\psi_{i+1,j}^{n+1,r} - \psi_{i,j}^{n+1,r}) \right\} \quad (I-2)$$

$$T_{i,j}^{n+1,r} = \frac{w\Delta t}{\Delta z^2} \left\{ -K_{II}^{n+1,r} + \frac{D_{i,j}^{n+1,r}}{2} (\psi_{i,j}^{n+1,r} - \psi_{i,j-1}^{n+1,r} - \Delta z) \right\} \quad (I-3)$$

$$B_{i,j}^{n+1,r} = \frac{w\Delta t}{\Delta z^2} \left\{ -K_{IV}^{n+1,r} - \frac{D_{i,j}^{n+1,r}}{2} (\psi_{i,j+1}^{n+1,r} - \psi_{i,j}^{n+1,r} - \Delta z) \right\} \quad (I-4)$$

$$P_{i,j}^{n+1,r} = C_{i,j}^{n+1,r} + \frac{w\Delta t}{\Delta x^2} \left\{ K_{III}^{n+1,r} - \frac{D_{i,j}^{n+1,r}}{2} (\psi_{i+1,j}^{n+1,r} - \psi_{i,j}^{n+1,r}) + K_I^{n+1,r} + \frac{D_{i,j}^{n+1,r}}{2} (\psi_{i,j}^{n+1,r} - \psi_{i-1,j}^{n+1,r}) \right\} \\ + \frac{w\Delta t}{\Delta z^2} \left\{ -K_{IV}^{n+1,r} - \frac{D_{i,j}^{n+1,r}}{2} (\psi_{i,j-1}^{n+1,r} - \psi_{i,j}^{n+1,r} - \Delta z) + K_{II}^{n+1,r} + \frac{D_{i,j}^{n+1,r}}{2} (\psi_{i,j}^{n+1,r} - \psi_{i,j-1}^{n+1,r} - \Delta z) \right\} \quad (I-5)$$

$$\text{Res}_{i,j}^{n+1,r} = \theta_{i,j}^{n+1,r} - \theta_{i,j}^n \\ + \frac{w\Delta t}{\Delta x} \{ V_{III}^{n+1,r} - K_I^{n+1,r} \} + \frac{(1-w)\Delta t}{\Delta x} \{ V_{III}^{n,r} - V_I^{n,r} \} \\ + \frac{w\Delta t}{\Delta z} \{ V_{IV}^{n+1,r} - V_{II}^{n+1,r} \} + \frac{(1-w)\Delta t}{\Delta z} \{ V_{IV}^{n,r} - V_{II}^{n,r} \} \quad (I-6)$$

Notations

- C_n : Courant number;
 d : root zone depth (cm);
 $E_a(0,t)$: actual evapotranspiration (cm);
 $f(t)$: relative humidity of the air (fraction);
 g : acceleration due to gravity (m/s);
 h : flow depth (m);
 h_{ini} : depth of flow for the initial condition (m);
 I : volumetric rate of infiltration per unit area (m/s);
 K : the consumptive use coefficient (defined as the ratio of evapotranspiration to Pan evaporation, E_p);
 $K(\psi)$: unsaturated hydraulic conductivity (cm/hr);
 K_s : saturated hydraulic conductivity (cm/hr);
 M : the molecular weight of water (18 gm/mole);
 n : manning roughness coefficient ;
 q : discharge per unit width (m^3/s per unit width);
 q_{ini} : discharge specified as the initial condition (m^3/s per unit width);
 q_{uns} : discharge specified at u/s end (B.C.);
 R : the universal gas constant ($8.314 \text{ H } 10^7 \text{ erg/mole/K}$);
 S_o : slope of the irrigated field border;
 S_f : friction slope;
 S_i : Sink term (rate of withdrawal of water per unit volume of the soil (cm/hr));
 $T(t)$: the absolute temperature (K);
 t : time (s);
 $t_a(i)$: time of arrival of the wetting front at node i ;
 $t_a(n-1)$: time of arrival of the wetting front at D/S end;
 t_{shut} : time to shutoff;
 V_x : Darcy flow velocity in the x direction (m/s);
 V_z : Darcy flow velocity in the z direction (m/s);
 w : time weighting factor;
 x & z : distances along the x & z coordinate directions (m);
 ψ : pressure head (m);
 ψ_b : imposed pressure head at the ground surface;
 ψ_1 : pressure head at first grid under the ground;
 ψ_2 : pressure head at second grid under the ground;
 θ : volumetric moisture content;
 θ_{an} : moisture content at anaerobiosis point (at $\psi = -50$ cm);
 θ_d : moisture content at $\psi = -400$ cm;
 θ_{ini} : initial moisture content;
 θ_r : residual moisture content;
 θ_s : saturated moisture content;
 θ_w : moisture content at wilting point (at $\psi = -15800$ cm);
 Δx : grid size in x -direction;
 Δz : grid size in z -direction;
 Δt : time stepping;

- α : a positive coefficient
- γ : the weight coefficient;
- ε : convergence tolerance.

Superscripts

- $n, n+1$: refers to the values of the variables at known and unknown time levels;
- r : superscript denotes the iteration number;

Subscripts

- i : refer to the grid point in x-direction;
- j : refer to the grid point in z-direction;
- s : refer to the side face of the domain.

Director : Dr. K. S. Ramasastri

Divisional Head : Dr. V. K. Choubey, Scientist 'E'

Study Group : Dr. Vivekanand Singh, Scientist 'B'